GEOPHYSICS, VOL. 67, NO. 5 (SEPTEMBER-OCTOBER 2002); P. 1586–1592, 6 FIGS.
10.1190/1.1512804

Short Note

Multifocusing imaging with controlled reflection-point dispersal

Boris Gurevich* and Evgeny Landa‡

INTRODUCTION

Multifocusing imaging proposed by Gelchinsky (Gelchinsky et al., 1999a, b; Landa et al., 1999) belongs to a group of techniques that can be characterized as macro-model independent imaging methods. These methods, which also include the common-reflection surface method (Mann et al., 1999; Jäger et al., 2001), and optical stack (de Bazelaire, 1988), are described in a collection of papers published as a special issue of the *Journal of Applied Geophysics* (Hubral, 1999). Macro-model independent imaging methods represent a new alternative to the classical processing sequence of NMO, dip moveout (DMO), and stacking. They are based upon a new transformation of 2-D multicoverage prestack data into a simulated zero-offset stack section. This transformation involves stacking large supergathers of seismic traces, each of which can span many common-midpoint (CMP) gathers. Stacking of large supergathers is made possible by the use of a generalized moveout correction. For a given source-receiver pair, this correction depends on three parameters: the wavefront curvatures of the normal wave, the normal incidence point wave (Hubral, 1983), and the emergence angle of the central ray. For each supergather and each zero-offset time, T_0, these parameters are obtained through a coherence analysis of the moveout corrected supergather.

The primary advantage of the multifocusing method is the enhancement of the signal-to-noise ratio of stacked sections through stacking of a much larger number of traces than in conventional CMP stacking. In general, this effect is stronger for larger supergathers. However, using large supergathers raises the question of spatial resolution. Because the multifocusing moveout correction is based on the spherical approximation of wavefronts, it automatically takes into account the dip and curvature of the reflector. Therefore, in contrast to conventional NMO supergather processing, different traces in the supergather are stacked with their individual time shifts, which depend not only on the source-receiver offset, but also on the position of the midpoint with respect to the central trace in the supergather. Thus, multifocusing stacking does not suffer from a severe loss of spatial resolution, typical for conventional supergather velocity analysis. In particular, multifocusing moveout correction is exact for a single dipping reflector under a homogeneous overburden (irrespective of the dip), and accurate to fourth order in source-receiver offset for any smooth reflector that can be adequately approximated by a two-term power series (i.e., by an arc of constant curvature) in the area where reflection points corresponding to the traces of the supergather are located. However, if these conditions are violated, such as in the presence of a fault or by abrupt changes in the overburden, the spherical approximation of wavefronts is no longer valid, and multifocusing stacking may smooth out sharp discontinuities in the reflector.

An obvious way to avoid this smoothing effect is to use smaller supergathers. However, because of the reflection-point dispersal, the area of reflection points on a given reflector may be relatively large even for different traces from a single CMP gather. Conversely, because of the same dispersal effect, reflections from a given element of the reflector would belong to nonadjacent CMP gathers, and would not be stacked together.

In this paper, we show an alternative approach to this problem, based on the stacking of large supergathers while maintaining good spatial resolution. This effect is achieved by limiting the extent of the area of reflection points on a given reflector (subsurface aperture), rather than limiting the range of CMPs (surface aperture) as in the case of small supergathers. The analysis is performed for a homogeneous overburden, but may be extended to the inhomogeneous case using the concept of an auxiliary medium (Perroud et al., 1999; Jäger et al., 2001).

MOVEOUT CORRECTION IN MULTIFOCUSING IMAGING

Let us first consider acquisition on a flat surface (Figure 1). The central ray starts at C (which is referred to as the central point) with an angle β to the downward vertical (measured

Manuscript received by the Editor November 27, 2000; revised manuscript received February 21, 2002.
*Formerly The Geophysical Institute of Israel, Lod 71100, Israel; presently Curtin University of Technology, Department of Exploration Geophysics, GPO Box U1987, Perth, Western Australia 6845. E-mail: gurevich@geophy.curtin.edu.au.
‡Formerly, The Geophysical Institute of Israel, Post Office Box 182, Lod 71100, Israel; presently, OPERA, University of Pau, France. E-mail: evgeny.landa@univ-pau.fr.

clockwise). It hits the reflector Σ at the normal incidence point N, and returns to C. A paraxial ray from the source, S, hits the reflector, Σ, at R, intersects the central ray at P and arrives back at the surface at the receiver location G. These two rays define a fictitious focusing wave which initially has the wave front Σ_S, is returned by the reflector Σ, focuses at P, and emerges again at C with the wave front Σ_G. The traveltime difference between the paraxial ray *SRG* and the central ray *CNC* (the so-called multifocusing moveout) can be written (Gelchinsky et al., 1999a; Landa et al., 1999) as

$$\Delta\tau = \Delta\tau^+ + \Delta\tau^-, \tag{1}$$

where

$$\Delta\tau^+ = \frac{\sqrt{(R^+)^2 + 2R^+X_S\sin\beta + X_S^2} - R^+}{V_0} \tag{2}$$

is the traveltime difference between the *SRP* section of the paraxial ray and the corresponding *CNP* section of the central ray. Then,

$$\Delta\tau^- = \frac{\sqrt{(R^-)^2 + 2R^-X_G\sin\beta + X_G^2} - R^-}{V_0} \tag{3}$$

is the traveltime difference between the *PG* section of the paraxial ray and the corresponding *PC* section of the central ray. Here,

$$R^+ = \frac{1+\sigma}{\dfrac{1}{R_{\rm N}} + \dfrac{\sigma}{R_{\rm NIP}}}, \tag{4}$$

$$R^- = \frac{1-\sigma}{\dfrac{1}{R_{\rm N}} - \dfrac{\sigma}{R_{\rm NIP}}}, \tag{5}$$

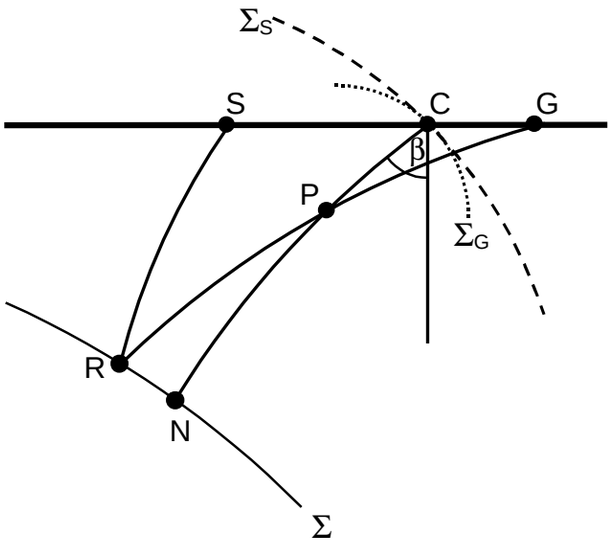

FIG. 1. Ray diagram of multifocusing moveout correction from a flat surface.

and σ is the so-called focusing parameter given by

$$\sigma = \frac{X_S - X_G}{X_S + X_G + 2\dfrac{X_SX_G}{R_{\rm NIP}}\sin\beta}. \tag{6}$$

In the above equations, X_S and X_G are the source and receiver offsets for a given ray with respect to the central ray, R^+ and R^- are the radii of curvature of the fictitious wave fronts Σ_S and Σ_G in the vertical plane, respectively, and V_0 is the near surface velocity which is assumed to be constant along the surface. Finally, $R_{\rm N}$ and $R_{\rm NIP}$ denote the radii of curvature of the two fundamental wave fronts, corresponding to the normal (N) wave and normal incidence point (NIP) wave, respectively (Hubral, 1983). The wavefront of the normal wave is formed by normal rays emitted by different points on the reflector (as in an "exploding reflector" concept). The NIP wavefront is formed by a point source placed at the point where the zero-offset ray, emitted from the central point, reaches the reflector. The double square root in equation (1) can be understood using the concept of an auxiliary medium (Perroud et al., 1999; Cruz et al., 2000) which can be defined as a homogeneous medium with the velocity equal to the near-surface velocity V_0. In the auxiliary medium both the central and paraxial rays are represented by combinations of straight line segments.

It is clear from Figure 1 that, for a given central ray, the radii of the fictitious wavefronts, R^+ and R^-, depend upon the position of the point P where the paraxial ray intersects the central ray, and thus upon the position of the source and receiver that define the paraxial ray. Equations (4) and (5) give the radii of curvature of these fictitious wavefronts in terms of the fundamental radii of curvature $R_{\rm N}$ and $R_{\rm NIP}$, which are defined by the central ray only and are the same for all the source-receiver pairs in the vicinity of the central ray. The dependence of the radii R^+ and R^- on the position of the source and receiver (or on the position of the point P on the central ray) is contained in the focusing parameter σ, which has a very clear physical interpretation. In particular, $\sigma = 0$ means that $R^+ = R^- = R_{\rm N}$, which implies that P coincides with the center of curvature of the normal wavefront (or of the reflector), and corresponds to the case of coinciding source and receiver (zero-offset configuration). The case $\sigma = 1$ ($\sigma = -1$) implies $R^- = 0$ ($R^+ = 0$), and corresponds to the situation where the central point coincides with the source (receiver) location. When $\sigma = \infty$, then $R^+ = R^- = R_{\rm NIP}$, and this is the situation where the focusing point P coincides with N.

REFLECTION POINT DISPERSAL FOR A DIPPING REFLECTOR

Generally speaking, the reflection point dispersal is a function of both NIP- and N-wave radii. Here, we illustrate the derivation of the dispersal for a flat dipping reflector ($R_{\rm N} = \infty$) under a homogeneous overburden (Figure 2). For a nonhomogeneous overburden, this derivation corresponds to the reflection point dispersal in the so-called auxiliary medium (Perroud et al., 1999).

Let x_0 be the horizontal coordinate of the central point C; x_S and x_G coordinates of the source S and receiver G, respectively; and let origin O be the intersection of the reflector Σ with

the observation surface. We define $X_S = x_S - x_0$, $X_G = x_G - x_0$ as signed source and receiver offsets from the central trace, respectively. The reflection-point dispersal δ for a given paraxial ray SRG with respect to a given central ray CN is defined as the distance between the reflection points R and N:

$$\delta = RN = |AN - AR|,$$

where point A is the projection of the source S onto the reflector, and

$$AR = SA \tan\gamma = OS \sin\beta \tan\gamma = x_S \sin\beta \tan\gamma$$
$$= (x_0 + X_S) \sin\beta \tan\gamma, \quad (7)$$

where γ is angle of incidence of the paraxial ray and β the emergence angle of the central ray. Noting that the one-way length of the normal ray CN is R_{NIP} and

$$x_0 = R_{\mathrm{NIP}} / \sin\beta,$$

we rewrite AR in the form

$$AR = (R_{\mathrm{NIP}} + X_S \sin\beta) \tan\gamma. \quad (8)$$

The distance AN can be written as

$$AN = -X_S \cos\beta$$

(note that in Figure 2 offset X_S is negative), so that

$$\delta = |AN - AR| = |(R_{\mathrm{NIP}} + X_S \sin\beta) \tan\gamma + X_S \cos\beta|. \quad (9)$$

Thus, in order to obtain δ, we need to express the incidence angle γ in terms of the source and receiver offsets, X_S and X_G. Similarly to equation (8), we can write

$$RB = (R_{\mathrm{NIP}} + X_G \sin\beta) \tan\gamma,$$

so that

$$AB = AR + RB = [2R_{\mathrm{NIP}} + (X_S + X_G) \sin\beta] \tan\gamma.$$

On the other hand,

$$AB = (X_G - X_S) \cos\beta.$$

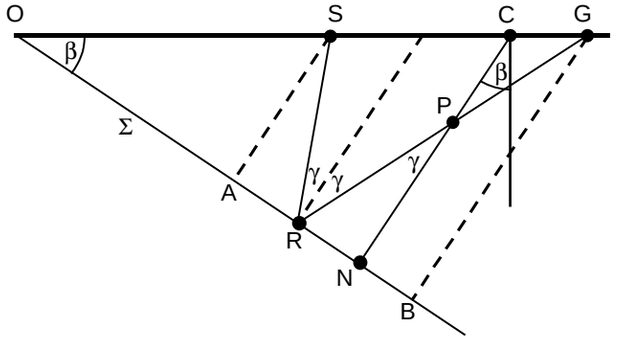

FIG. 2. Reflection-point dispersal for a flat dipping reflector.

Thus,

$$\tan\gamma = \frac{(X_G - X_S)\cos\beta}{2R_{\mathrm{NIP}} + (X_S + X_G)\sin\beta}. \quad (10)$$

Substitution of $\tan\gamma$ into equation (9) yields

$$\delta = \left| \frac{X_G + X_S + \dfrac{2X_G X_S}{R_{\mathrm{NIP}}} \sin\beta}{2R_{\mathrm{NIP}} + (X_S + X_G)\sin\beta} \right| R_{\mathrm{NIP}} \cos\beta. \quad (11)$$

DISPERSAL CONTROL IN MULTIFOCUSING IMAGING

Equation (11) can be used to control the reflection-point dispersal. In multifocusing imaging, a supergather is formed for each central trace, and for each sample on the central trace optimal values of moveout parameters β, R_{NIP}, and R_{N} are found to be those values that maximize the coherence criterion computed over the supergather after multifocusing moveout (MFMO) correction. In a standard multifocusing algorithm, the coherence of the MFMO-corrected supergather is evaluated by computing the semblance value for samples taken from all traces contained in the supergather. If we wish to restrict the reflection point dispersal by a given threshold value d, we can, for a given sample and a given combination of moveout parameters, include in the semblance calculations trace segments only from traces that satisfy the condition

$$\frac{\delta}{\cos\beta} < d,$$

or

$$\left| \frac{X_G + X_S + \dfrac{2X_G X_S}{R_{\mathrm{NIP}}} \sin\beta}{2R_{\mathrm{NIP}} + (X_S + X_G)\sin\beta} \right| R_{\mathrm{NIP}} < d \quad (12)$$

(here $\delta/\cos\beta$ represents the normal projection of δ onto the surface along the normal ray). Therefore, we would include in the coherence analysis only those traces within the supergather that correspond to rays with a reflection point within the distance d from the reflection point of the normal ray. We call parameter d the subsurface aperture.

The control over reflection-point dispersal enhances the flexibility of the multifocusing method through the choice of the control parameter d. If multifocusing imaging is performed with supergathers consisting of n CMP gathers, parameter d may be chosen within the interval

$$0 \le d \le n\Delta x,$$

where Δx is the interval between adjacent CMPs. The choice $d = n\Delta x$ means no reflection-point control. Conversely, choosing d to be very small ($\le \Delta x$) means that only trace segments containing reflections from a minimal area around the normal incidence point are included in the calculations.

The choice of an optimal subsurface aperture is related to the spatial resolution of the seismic data, which is defined by

several factors such as the size of the Fresnel zone, and the signal-to-noise ratio in the data. If the noise level in prestack data is high, one may wish to use a larger subsurface aperture, up to $d = n\Delta x$, to increase the stacking power even at the expense of a lower resolution. If, on the other hand, the signal-to-noise ratio is sufficiently high, smaller values of d corresponding to the size of the Fresnel zone can be used to achieve the highest resolution. Detailed investigation of these relationships is beyond the scope of the geometrical-acoustical analysis of this paper.

Control over reflection point dispersal in multifocusing imaging offers two potential advantages. First, if d is sufficiently small, the effect of reflector curvature may be ignored. In other words, if reflection points are located close to the normal incidence point, the reflector in this vicinity can be approximated by a straight line segment, which corresponds to an infinite normal-wave radius. Therefore, the MFMO correction can be accurately approximated by taking the normal-wave radius to be infinite, i.e., $R_N = \infty$. This greatly simplifies the coherence analysis by reducing the number of search parameters from three to two: β and R_{NIP}.

Secondly, control over the subsurface aperture can minimize an unwanted oversmoothing of the reflection events on the stacked section, and the corresponding loss of spatial resolution. This keeps the stacking aperture within the limits of the spherical approximation of the wavefronts. The smaller the subsurface aperture, the higher the spatial resolution. This effect is explained in the next section, where we show that, in the limit of small d, the multifocusing with controlled dispersal is equivalent to the common reflecting element (CRE) method. In turn, the CRE method is known to have spatial resolution equivalent to, or higher than, that in a DMO stack (Cruz et al., 2000). The relationship between multifocusing and CRE methods is discussed in the next section.

MULTIFOCUSING WITH CONTROLLED DISPERSAL AND CRE METHOD

To gain further insight into the above results, we now show that for $d = 0$ the multifocusing procedure reduces to the CRE method (Gelchinsky, 1988; Rabbel et al., 1991; Perroud et al., 1999; Cruz et al., 2000). Indeed, if $d = 0$, it follows from equation (11) that

$$X_G + X_S + \frac{2X_G X_S}{R_{NIP}} \sin\beta = 0, \tag{13}$$

or, in midpoint/half-offset coordinates $m = (X_G + X_S)/2$, $h = (X_S - X_G)/2$,

$$m + \frac{m^2 - h^2}{R_{NIP}} \sin\beta = 0. \tag{14}$$

Solving equation (14) for m yields

$$m = \frac{1}{2\alpha}\left(1 - \sqrt{1 + 4\alpha^2 h^2}\right), \tag{15}$$

where $\alpha = -\sin\beta / R_{NIP}$. Equation (15) is identical to the equation for the midpoint position in a common reflection point (CRP) gather (Perroud et al., 1999) and to the definition of the so-called CRE gather in the CRE method (Gelchinsky, 1988; Cruz et al., 2000), which comprises the events reflected from the same element of the reflector. Equation (15) could also be obtained directly from Levin's formula for the reflection point displacement in a single CMP (Levin, 1971),

$$m = \frac{h^2}{D} \sin\beta; \tag{16}$$

a function which is widely used in the analysis of dip moveout (Deregowski, 1982). In equation (16) $D = R_{NIP} + m \sin\beta$ denotes the distance between the midpoint at half-offset h and the (flat) reflector. Furthermore, it follows from equation (13) that the parameter σ given by equation (6) is infinite. Thus $R^+ = R^- = R_{NIP}$, and the moveout correction (1) reduces to

$$\Delta\tau = \Delta\tau^+ + \Delta\tau^-, \tag{17}$$

where

$$\Delta\tau^+ = \frac{\sqrt{(R_{NIP})^2 + 2R_{NIP}X_S \sin\beta + X_S^2} - R_{NIP}}{V_0} \tag{18}$$

$$\Delta\tau^- = \frac{\sqrt{(R_{NIP})^2 + 2R_{NIP}X_G \sin\beta + X_G^2} - R_{NIP}}{V_0}, \tag{19}$$

which is equivalent to the moveout correction in the CRE method.

Therefore, multifocusing with zero reflection-point dispersal is equivalent to the CRE method. Moreover, multifocusing with small but nonzero dispersal represents a straightforward generalization of the CRE method which may have some useful advantages. The advantages of using multifocusing with d of the order of a few CMP intervals instead of the CRE method can be summarized as follows.

Trace interpolation is not necessary.—In order to be included in CRE gather, the source and receiver coordinates of an individual trace have to obey equations (13) or (15). However, since in reflection seismology the observation systems are discrete, for a given half-offset h a trace with a midpoint coordinate $x_0 + m(\alpha, h)$ may not exist. Thus, in order to build a CRE gather, it is necessary either to take a trace from a nearest-neighbor midpoint (for which CRE traveltime equations are approximate), or to use trace interpolation, a complicated task in itself. Using nonzero reflection-point dispersal d relaxes equation (13) to the inequality (12), which in midpoint/half-offset coordinates is

$$m + \alpha(h^2 - m^2) < d(1 - m\alpha). \tag{20}$$

Thus, rather than building a CRE gather from traces that approximately satisfy equation (13), we may build a generalized CRE gather by including in it all traces that satisfy the inequality (20). In particular, choosing d to be equal to a single CMP interval would make up a generalized CRE gather with the same number of traces as in a CMP gather. Of course,

strictly speaking, for the generalized CRE gather the standard CRE moveout equations (17)–(19) are no longer valid, and the full multifocusing moveout given by equations (1)–(3) must be used. However, as mentioned before, as d is relatively small (e.g., $d \ll R_{\rm NIP}$), the normal-wave radius R_N may be assumed to be infinite. Thus, the generalized CRE method involves the same two moveout parameters, $R_{\rm NIP}$ and β, as the standard CRE method.

Increased stacking power.—Making d equal to several CMP intervals may result in a greater stacking power and an increase in signal-to-noise ratio compared to standard CRE or CMP methods.

Unlocking the strong coupling between the CRE parameters.—A more fundamental difficulty in the standard CRE method is associated with the strong coupling between two CRE parameters, $R_{\rm NIP}$ and β, or between $R_{\rm NIP}$ and $\alpha = -\sin\beta/R_{\rm NIP}$. In other words, for a given reflection event, and for any given trial value of $\alpha = \alpha_1$, there exist a $R_{\rm NIP}$ value R_1 that yields in the CRE gather defined by α_1 a moveout curve, which is identical to the true traveltime curve in that CRE gather up to second order in offset. This effect is similar to the coupling between the overburden velocity and dip in the standard NMO equation.

The difference between these two effects lies in the fact that while in standard NMO this coupling is exact, in CRE processing the coupling is only up to second order in offset. However, since small and medium offsets usually constitute a large portion of seismic data (as evident from the large range of validity for the parabolic traveltime approximation), a large area of uncertainty in the (α, $R_{\rm NIP}$) domain would always be present in the CRE method. Thus, in the CRE method, the parameters α, $R_{\rm NIP}$ are ill conditioned.

However, if, instead of using the CRE method, which is equivalent to the multifocusing method with $d = 0$, we assume a nonzero value for d, the poor conditioning is easily unlocked. Indeed, whereas in the CRE method only one trace [defined by equation (15)] is included in the CRE gather for each half-offset h, setting $d > 0$ allows for a nonzero range of midpoints for each h, as defined by the condition (20). In particular, for zero or very small offsets $h \ll R_{\rm NIP}$, the condition (20) reduces to a simple inequality $m < d$. For example, if $d = n\Delta x$, where Δx is the CMP interval, then the generalized CRE gather would contain n traces for each small half-offset h. For the same very small offsets and d in the range $0 < d \ll R_{\rm N}$, the traveltime is given by

$$t = t_0 - \frac{2\sin\beta_0}{v_0} m, \tag{21}$$

from which $\sin\beta$ can be easily estimated by a linear regression, thereby unlocking the ambiguity between the CRE parameters $R_{\rm NIP}$ and $\alpha = -\sin\beta/R_{\rm NIP}$. This procedure is just a demonstration of how the parameter ambiguity is resolved. In practice, there is no need to select minimum offset traces. The CRE parameters may be estimated in a single step by the multifocusing procedure with $d \geq 2\Delta x$.

We illustrate this important feature of the generalized CRE method on synthetic data computed for a simple model shown in Figure 3. The primary-only reflection data were generated by ray tracing for 160 midpoints with a 25-m CMP interval and offsets between 25 and 2400 m. A certain amount of random noise was added to the data, as can be observed on the minimum offset section shown in Figure 4.

Figures 5 and 6 show the estimates of two multifocusing (or CRE) attributes: the emergence angle and NIP-wave radius. The sections in Figures 5a and 6a were obtained with a subsurface aperture d equal to the CMP interval (25 m). As shown in the above analysis, this is approximately equivalent to the CRE method. Figures 5b and 6b show the same attributes obtained with d equal to 9 CMP intervals (225 m). In both cases the multifocusing analysis was performed on supergathers consisting of 30 CMP gathers each. Although both algorithms perform similarly on such a simple model, the difference in the stability of the parameter estimation is quite dramatic. The estimates in Figures 5a and 6b are very much unstable due to the coupling between the emergence angle and the NIP radius in the CRE method, and in multifocusing with a very small (compared to the target depth) subsurface

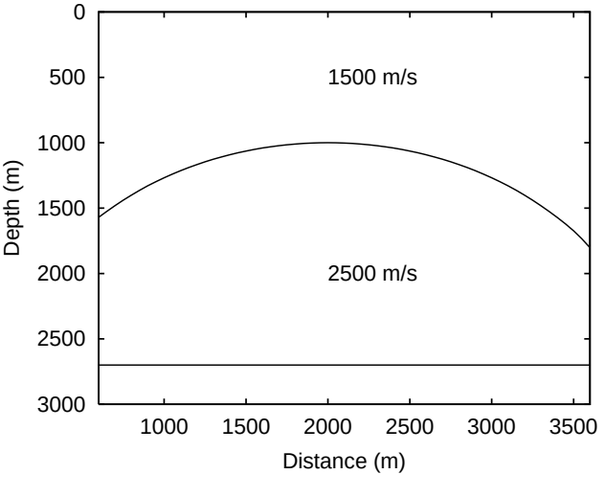

FIG. 3. Geometry of the seismic model.

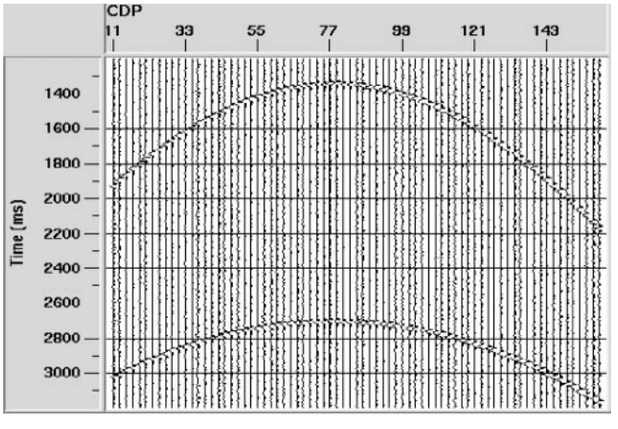

FIG. 4. Minimum offset section corresponding to the model in Figure 3.

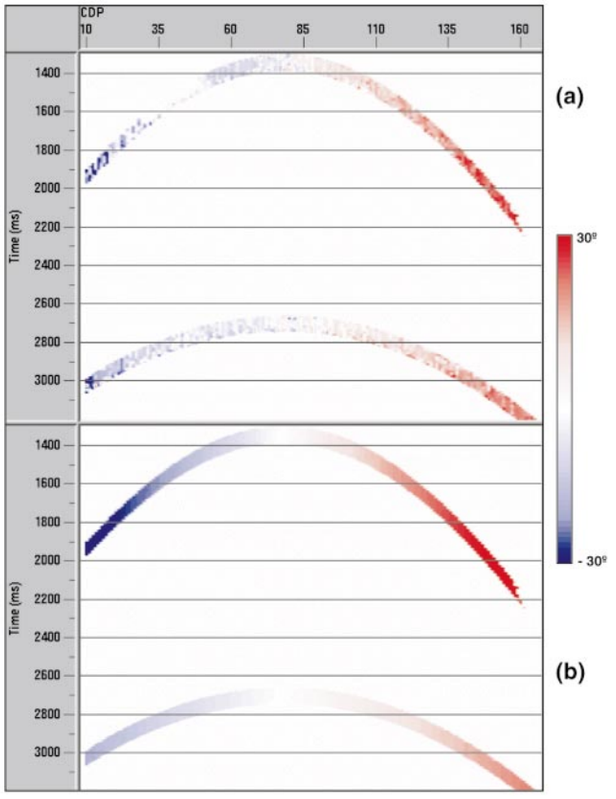

FIG. 5. Emergence angle estimates for two interfaces from the multifocusing analysis (a) with the subsurface aperture $d = 1$ CMP interval, and (b) with $d = 9$ CMP intervals. The multifocusing with a small d, which is approximately equivalent to the CRE method, results in a less robust estimation than that with the larger d.

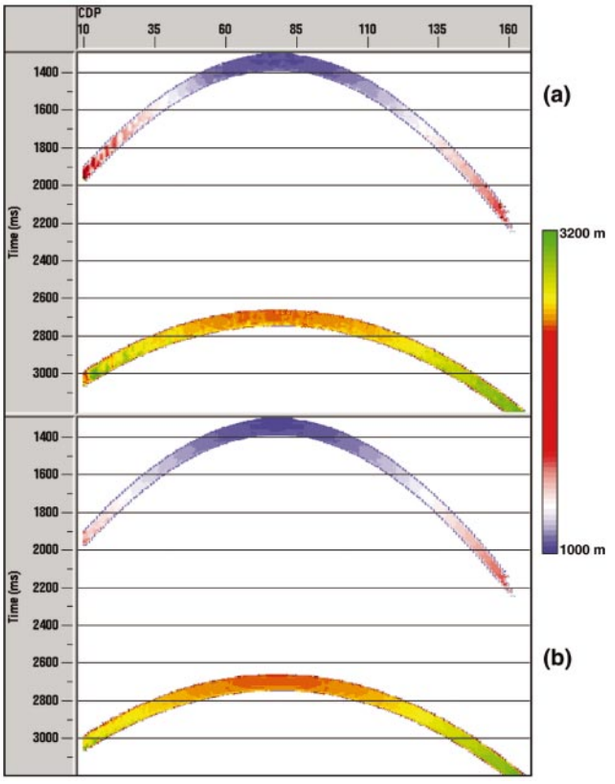

FIG. 6. Estimates of the NIP-wave radius for two interfaces from the multifocusing analysis (a) with the subsurface aperture $d = 1$ CMP interval, and (b) with $d = 9$ CMP intervals. The multifocusing with a small d, which is approximately equivalent to the CRE method, results in a less robust estimation than that with the larger d.

aperture d. As explained above, Figures 5b and 6b demonstrate that this coupling can be unlocked by using a larger subsurface aperture d.

CONCLUSIONS

We have presented a modification of the multifocusing method of seismic imaging based on the stacking of large supergathers while maintaining good spatial resolution. This effect is achieved by limiting the extent of the area of reflection points on a given reflector (subsurface aperture or reflection-point dispersal d).

The control over the reflection-point dispersal in multifocusing imaging has two straightforward advantages. First, if d is chosen sufficiently small, the effect of reflector curvature may be ignored, and the MFMO correction may be accurately approximated by taking the normal-wave radius to be infinite. This greatly simplifies the coherence optimization by reducing the number of search parameters from three to two: the emergence angle and NIP-wave radius. Secondly, the control over the subsurface aperture prevents an oversmoothing of the reflection events on the stacked section, and a corresponding loss of spatial resolution, by keeping the stacking aperture within the limits of the spherical approximation of wavefronts.

Multifocusing with $d \to 0$ has been shown to be equivalent to the CRE method. In addition, we have shown that using small (on the order of a few CMP intervals) values of d presents certain advantages over the CRE method. In particular, it (1) avoids trace interpolation, (2) increases the stacking power, and (3) unlocks the strong coupling between the emergence angle and the NIP radius.

ACKNOWLEDGMENTS

The research was carried out with the support of the Israel Ministry of National Infrastructures. One of the authors (EL) thanks the Univeristy of Pau, France, for partial support of this work during his stay at the university in 2000. We also thank Shemer Keydar and Moshe Reshef for useful discussions, and John A. McDonald for editing the manuscript.

REFERENCES

Cruz, J. C. R., Hubral, P., Tygel, M., Schleicher, J., and Höcht, G., 2000, The common reflecting element (CRE) method revisited: Geophysics, **65**, 979–993.

de Bazelaire, E., 1988, Normal moveout revisited—Inhomogeneous media and curved interfaces: Geophysics, **53**, 143–157.

Deregowski, S. M., 1982, Dip moveout and reflector point dispersal: Geophys. Prosp., **30**, 318–322.

Gelchinsky, B., 1988, The common-reflecting-element (CRE) method (non-uniform asymmetric multifold system): Expl. Geoph., **19**, 71–75.

Gelchinsky, B., Berkovitch, A., and Keydar, S., 1999a, Multifocusing homeomorphic imaging: Part 1: Basic concepts and formulae: J. Appl. Geoph., **42**, 229–242.

——— 1999b, Multifocusing homeomorphic imaging: Part 2: Multifold data set and multifocusing: J. Appl. Geoph., **42**, 243–260.

Hubral, P., 1983, Computing true amplitude reflections in a laterally inhomogeneous earth: Geophysics, **48**, 1051–1062.

——— Ed., 1999, Macro-model independent seismic reflection imaging: J. Appl. Geoph., **42**, 137–346.

Jäger, R., Mann, J., Höcht, G., and Hubral, P., 2001, Common-reflecting-surface stack: Image and attributes: Geophysics, **66**, 97–109.

Landa, E., Gurevich, B., Keydar, S., and Trachtman, P., 1999, Application of multifocusing method for subsurface imaging: J. Appl. Geoph., **42**, 283–300.

Levin, F. K., 1971, Apparent velocity from dipping interface reflections, Geophysics, **36**, 510–516.

Mann, J., Jäger, R., Müller, T., Höcht, G., and Hubral, P., 1999, Common-reflecting-surface stack—A real data example: J. Appl. Geoph., **42**, 301–318.

Perroud, H., Hubral, P., and Höcht, G., 1999, Common-reflection-point stacking in laterally inhomogeneous media: Geophys. Prosp., **47**, 1–24.

Rabbel, W., Buittner, R., and Gelchinsky, B., 1991, The common-reflecting-element (CRE) method (non-uniform asymmetric multifold system): Phys. Earth Plan. Internat., **67**, 200–210.